Angewandte Chemie International Edition

Angewandte International Edition Chemie

GDCh German Chemical Society

How to cite: *Angew. Chem. Int. Ed.* **2026**, e9524706
doi.org/10.1002/anie.9524706

RESEARCH ARTICLE

Proton Transfer Shuttle Mediated Dormant–Active Balance for Accelerated and Controlled Polymerization of *N*-Carboxyanhydrides

Jing Huang[2] | Haonan Sheng[3,4] | Jianjun Cheng[3,4] | Xingliang Liu[1]

[1]Department of Biomedical Engineering, School of Engineering, China Pharmaceutical University, Nanjing, Jiangsu, China | [2]School of Biomedical Engineering and Informatics, Nanjing Medical University, Nanjing, Jiangsu, China | [3]School of Engineering and Research Center for Industries of the Future, Westlake University, Hangzhou, Zhejiang, China | [4]Institute of Advanced Technology, Westlake Institute for Advanced Study, Hangzhou, Zhejiang, China

Correspondence: Jianjun Cheng (chengjianjun@westlake.edu.cn) | Xingliang Liu (liuxingliang@cpu.edu.cn)

Received: 30 January 2026 | **Revised:** 6 June 2026 | **Accepted:** 16 June 2026

Keywords: dormant–active equilibrium | *N*-carboxyanhydride | polypeptide | proton transfer

ABSTRACT

Since its inception in 2003, the concept of "reversible deactivation" to control chain propagation has emerged as a promising, though still evolving, strategy for precise polypeptide synthesis. Beyond a simple polymerization method, this concept is expected to promote unique reaction pathways. Nevertheless, achieving both rapid and well-controlled ring-opening polymerization of *N*-carboxyanhydrides through the equilibrium between dormant and active species is rare and challenging. In this study, we report a proton transfer shuttle-assisted strategy that accelerates chain growth via trifluoroacetic acid (TFA) /tetrabutylammonium acetate (TBAA) cooperative system. Central to this strategy is reversible acceptance and donation of proton, thereby shifting the dormant–active equilibrium without disrupting it. This modulation increases the proportion of active chain ends while maintaining control over rapid polymerization process. Moreover, cooperative TFA/TBAA catalysis has streamlined the synthesis of well-defined polypeptides, which are amenable to further chemical modifications. Control experiments and density functional theory calculations provide insights into the origin of controllability and critical role of TFA/TBAA in regulating the reversible deactivation equilibrium. Consequently, this work establishes a robust and efficient approach for accelerated yet controlled preparation of polypeptides and generates fundamental insights that advance understanding and application of the "reversible deactivation" concept for precision polypeptide synthesis.

1 | Introduction

Polypeptides which share backbone structures with proteins and peptides [1, 2], exhibit excellent biocompatibility and degradability, rendering them as important biomaterials in fields such as drug delivery and tissue engineering [3–12]. Ring-opening polymerization (ROP) of amino acid *N*-carboxyhydrides (NCA) is one of the most efficient strategies for the synthesis of polypeptides, especially those with high molecular weight and non-natural amino acids [13–17]. However, conventional polymerization of NCAs in *N*,*N*-dimethylformamide (DMF) usually takes days to finish [18], suffering from various side reactions including chain terminations, chain transfer, and water-induced NCA degradation [18, 19]. The development of accelerated polymerization in solvents with low dielectric constants (e.g., dichloromethane (DCM)) offered great opportunities to facilitate the ROP of NCAs [20, 21]. The fast polymerization kinetics outpaces various side reactions, enabling polymerization in the presence of moisture and even aqueous phase [22]. Nevertheless, the polymerization in DCM follows a two-stage behavior induced by the coil–helix

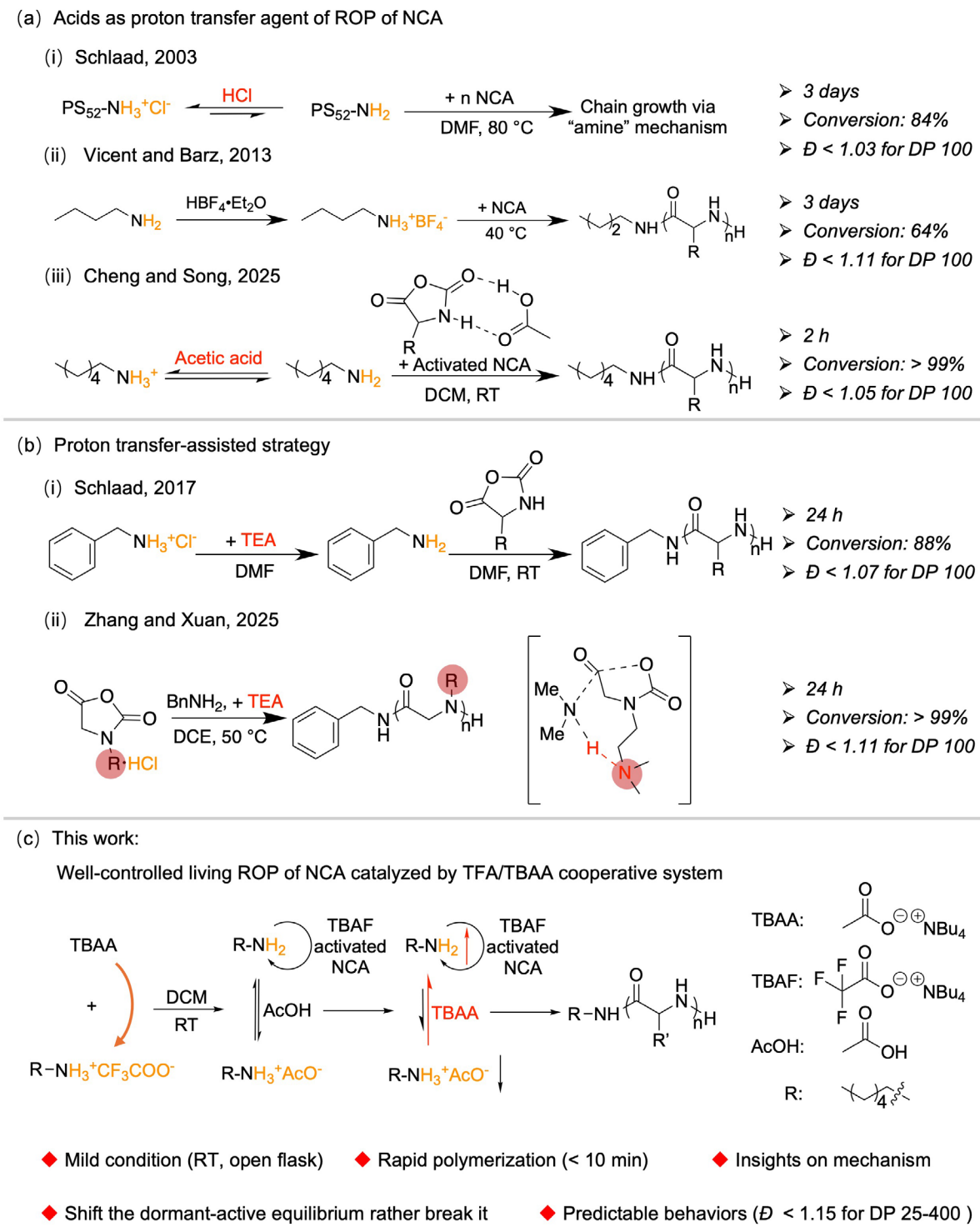

SCHEME 1 | Background and inspiration for the development of proton transfer shuttle-assisted ROP of NCA.

transition of the propagating chain, with the rate constant for the second stage 3 ~ 4 orders of magnitude higher than that of the first stage [20, 23]. Accordingly, polypeptides reaching the second stage would consume most monomers, while those remaining in the first stage would no longer propagate, which may result in polypeptides with elevated molecular weights (MWs).

Various efforts have been devoted to the synthesis of polypeptides with targeted MWs and narrow dispersity, including the developments of functional initiators and catalytic systems [17, 24–31]. Among these strategies, Schlaad and colleagues proposed primary amine hydrochlorides-initiated polymerization of NCAs, where primary amine hydrochlorides (—$NH_3^+Cl^-$) were considered as dormant species, whose dissociation released active primary amines and $H^+(Cl^-)$ (Scheme 1a) [24]. The latter would avoid side reactions such as activated monomer process and contribute to precise control over the polymerization in DMF. Additionally, Vicent and Barz reported that ammonium salts with non-nucleophilic tetrafluoroborate anions (BF_4^-) enabled synthesis of well-defined polypeptides, as BF_4^- diminished the

nucleophilicity of the anion and consequently suppressed activated monomer mechanism (AMM) (Scheme 1a) [27]. However, the protonation of most propagating primary amines, especially protonated by the strong acid HCl, left only a small amount of active polypeptide ends undergoing chain growth. This scarcity of active chain ends inherently slows down the polymerization kinetics, as evidenced by the prolonged reaction time of 3 days and a low monomer conversion of 84% [32].

To shift the equilibrium between dormant and active species, we previously applied weak acid, acetic acid (AcOH), to facilitate the controlled ROP of NCA, which should reversibly protonate primary amines while still maintaining sufficiently high amine chain-end reactivity (Scheme 1a) [33]. Current experimental evidence indicates that a saturated ionization level of the chain end was approximately 50% at $[AcOH]_0/[Initiator]_0 = 10$ [33]. To further accelerate the polymerization, proton transfer mechanism, which plays a central role in governing the kinetics of polymerization process, has been proposed to shift the equilibrium, increasing the proportion of active species [34–36]. Schlaad and colleagues reported a remarkable rate enhancement in primary ammonium-mediated ROP of NCA through the strategic incorporation of a proton shuttle catalyst triethylamine (TEA) (Scheme 1b) [24, 30]. TEA significantly increased the concentration of active centers and subsequently accelerated polymerization, while its strong basicity inevitably resulted in an undesired AMM [37]. Independent investigations by Zhang and colleagues proposed a side chain-assisted strategy, where TEA functioned as a proton modulator, facilitating the proton transfer from pendant tertiary ammonium to TEA for self-promoted polymerization (Scheme 1b) [38]. In these systems, TEA led to the complete release of primary amines/tertiary amines, which might break the equilibrium between active and dormant propagating chains in ROP of NCAs, precluding precise control over polymerization. Therefore, we hypothesized that proton shuttle catalyst that could reversibly accept and donate proton would shift the dormant–active equilibrium rather than break it, increasing the proportion of active chain ends while maintaining control over the rapid polymerization.

In this article, trifluoroacetic acid (TFA, with a low pka) was employed to protonate all nucleophilic amines, converting them into dormant species ($—NH_3^+CF_3COO^-$), which significantly enhanced the stability of NCA monomers. Subsequently, tetrabutylammonium acetate (TBAA) was introduced as a proton shuttle catalyst, which reacts with the dormant $-NH_3^+CF_3COO^-$, generating tetrabutylammonium trifluoroacetate (TBAF) while releasing an equivalent of both active amino species ($—NH_2$) and AcOH. The newly generated AcOH could reversibly protonate active amines and suppress the rate difference between the two stages. Meanwhile, the remaining TBAA further prompted rapid proton transfer shuttle between active ($—NH_2$) and dormant ($—NH_3^+AcO^-$) chain ends, promoting efficient regeneration of active centers (Scheme 1c). Additionally, TBAF should activate NCA monomers via hydrogen bonding, further accelerating the polymerization kinetics. This strategy facilitates rapid and controlled synthesis of polypeptides with predetermined degrees of polymerization (DP = 100) within 10 min, yielding products with narrow dispersity ($Đ < 1.05$). Moreover, the polymerization can be conducted under mild and ambient conditions without the need for anhydrous solvents, specially designed catalysts, Schlenk lines, or glove boxes. Density functional theory (DFT) calculations demonstrated that TBAA increased the energy barrier for the conversion from active to dormant species by assisting proton transfer process via a shuttle mechanism. Finally, polypeptide materials can be prepared in a rapid and controlled manner via modulation of intermolecular proton transfer shuttle processes.

2 | Results and Discussion

2.1 | Accelerated Polymerization in TFA/TBAA Cooperative System

In this work, we employed a TFA/TBAA cooperative system (Figure 1a) which not only maintained a reversible activation–deactivation equilibrium, but also leveraged TBAA as a proton shuttle catalyst to significantly increase the concentration of active centers. Initially, TFA was added to a DCM solution containing γ-benzyl-L-glutamate NCA (BLG-NCA) and hexylamine ($Hex\text{-}NH_2$) ($[M]_0 = 0.3$ M, $[M]_0/[I]_0/[TFA]_0 = 100:1:10$). Fourier transform infrared spectroscopy (FTIR) analysis confirmed the inhibition of polymerization for at least 5 days, evidenced by the absence of the amide bond signal of polypeptide at 1650 and 1548 cm^{-1}(Figure S1). Moreover, no polymerization occurred even in the presence of $Hex\text{-}NH_2$ and water (Figures S2 and S3), confirming that all nucleophilic amines were fully protonated by TFA and maintained in a dormant state as $-NH_3^+$ species, which effectively prevented premature polymerization. More importantly, it established a uniform initiation point, allowing the polymerization to proceed synchronously upon subsequent introduction of the proton shuttle catalyst TBAA (Figure S4). FTIR analysis revealed the complete consumption of NCA monomers within 10 min after its addition, evidenced by the disappearance of NCA anhydride peaks at 1857 and 1790 cm^{-1} (Figure 1b). This rapid kinetics indicated that the dormant $—NH_3^+$ species were efficiently deprotonated by TBAA, and the regenerated active $-NH_2$ species subsequently initiated highly synchronized polymerization.

Additionally, the acceleration effect of TFA/TBAA cooperative system was dependent on the initial molar ratio of $[TBAA]_0$ to $[TFA]_0$ (Figure 1c). The polymerization at $[TBAA]_0/[TFA]_0 = 0.1$ or 0.5 proceeded at a much slower rate, achieving only ~25% BLG-NCA conversion after 100 min polymerization ($[M]_0 = 0.3$ M, $[M]_0/[I]_0/[TFA]_0 = 100:1:10$) owing to the formation of stabilized dormant species with remaining TFA. An increase in $[TBAA]_0/[TFA]_0 = 1$ led to approximately 95% conversion within 90 min, owing to the conversion of inhibitory TFA into catalytic AcOH. Further increase in $[TBAA]_0/[TFA]_0 = 1.5$ and 2 significantly accelerated the polymerization, with over 95% of NCA polymerized within 10 min (Figure 1c), originated from the remaining TBAA. According to the previous work, the acceleration effect of the system was dependent on the amount of the organic acid [33]. Therefore, we systemically investigated the influence of the initial $[TFA]_0/[I]_0$ on the polymerization kinetics with constant TBAA concentration (Figure 1d). Specifically, increasing $[TFA]_0/[I]_0$ from 1 to 5 decelerated the polymerization, owing to the suppression of TBAA-initiated polymerization, which has been reported to finish within 3 min [19]. Conversely, further increase in $[TFA]_0/[I]_0$ to 10 and 15 resulted in an acceleration of the polymerization, achieving 95% conversion

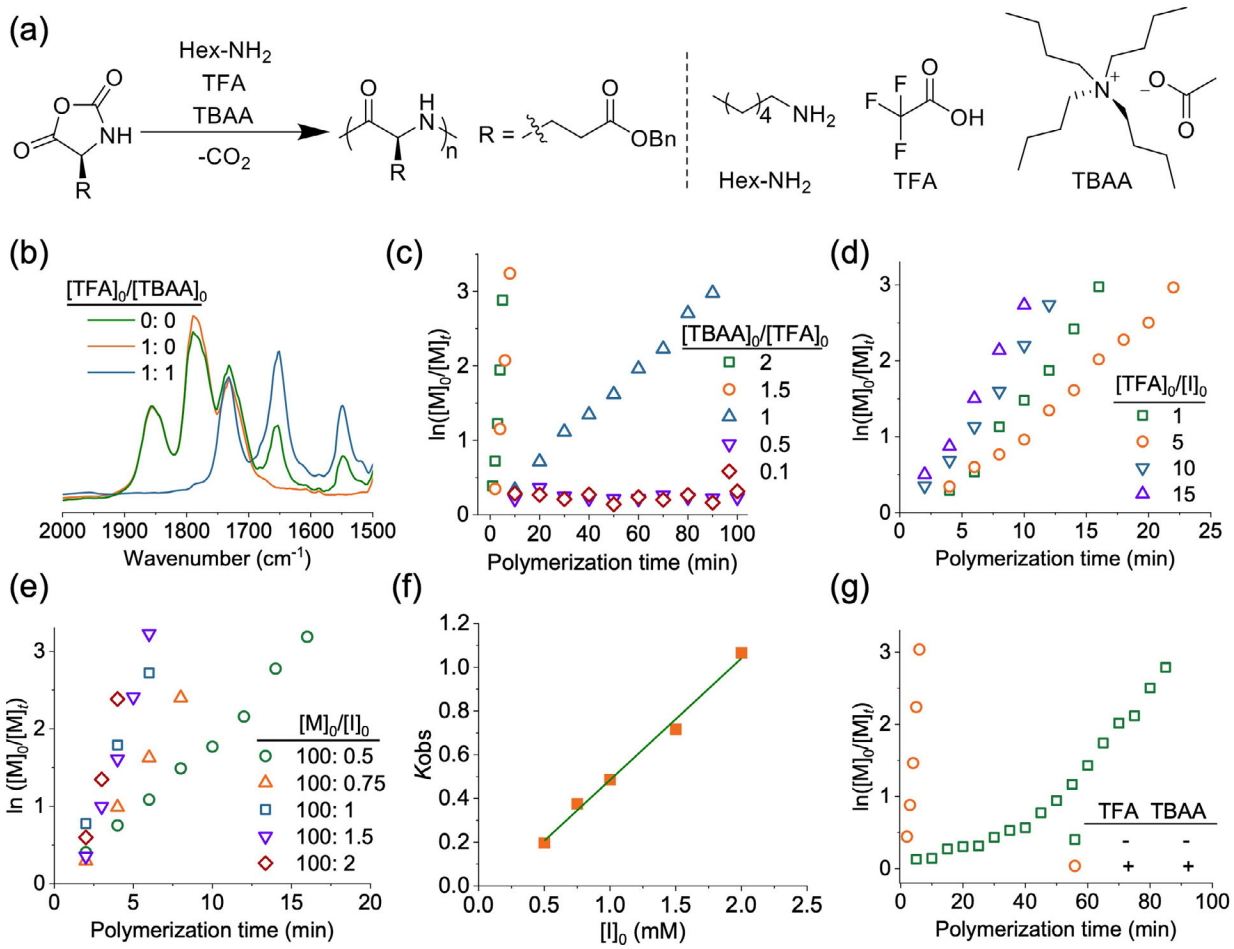

FIGURE 1 | The accelerated polymerization of NCAs in TFA/TBAA cooperative system. (a) Synthetic route of polypeptides in TFA/TBAA cooperative system. (b) Overlaid FTIR spectra showing the polymerization of BLG-NCA 10 min after initiation by Hex-NH_2 in the absence and presence of TFA/TBAA in DCM. $[M]_0/[I]_0/[TFA]_0/[TBAA]_0 = 100:1:10:15$, $[M]_0 = 0.3$ M. (c) Semilogarithmic kinetic plot of polymerization of BLG-NCA in DCM initiated by Hex-NH_2 at various $[TBAA]_0$. $[M]_0/[I]_0/[TFA]_0 = 100:1:10$, $[M]_0 = 0.3$ M. (d) Semilogarithmic kinetic plot of polymerization of BLG-NCA in DCM initiated by Hex-NH_2 at various $[TFA]_0$. $[M]_0/[I]_0/[TBAA]_0 = 100:1:15$, $[M]_0 = 0.3$ M. (e) Semilogarithmic kinetic plot of polymerization of BLG-NCA at various $[I]_0$, $[M]_0/[TFA]_0/[TBAA]_0 = 100:10:15$, $[M]_0 = 0.3$ M. (f) Plot of k_{obs} obtained from (e) versus $[I]_0$ and the linear fitting (green line, $R^2 = 0.992$) of the data. (g) Semilogarithmic kinetic plot of polymerization of BLG-NCA in DCM initiated by Hex-NH_2 in the presence and absence of TFA/TBAA. $[M]_0/[I]_0/[TFA]_0/[TBAA]_0 = 100:1:10:15$, $[M]_0 = 0.3$ M.

within merely 10 min (Figure 1d), likely due to the efficient conversion of inhibitory TFA into catalytic AcOH.

With the optimal $[TBAA]_0/[TFA]_0$ settled, the initiator concentration ($[I]_0$) was systematically varied to investigate its influence on the observed rate constant k_{obs} (Figure 1e). Kinetic analysis on TFA/TBAA cooperative polymerization system presented a linear correlation between k_{obs} and $[I]_0$, with a slope of 0.5561 ($R^2 = 0.992$) (Figure 1f), indicating a first-order kinetic, which is consistent with the characteristic of a living polymerization. In addition, $[M]_0$ also affected the polymerization kinetics, consistent with the previous studies of polymerization in DCM [21]. An increase in $[M]_0$ led to a substantial acceleration of the polymerization, with > 95% NCA consumed within 10 min in the presence of TFA and TBAA at $[M]_0 = 0.3$ and 0.4 M (Figure S5).

In contrast to previous reports on the cooperative covalent polymerization (CCP) in DCM [21, 23], the kinetic profile of the TFA/TBAA-accelerated polymerization did not display the characteristic two-stage kinetics which arose from a coil-to-helix conformational transition of propagating polypeptides at a critical DP of 8–12. Instead, the polymerization conducted at $[M]_0/[I]_0 = 100$ in TFA/TBAA cooperative system (Figure 1g) exhibited one-stage kinetics, whereas a clear two-stage kinetic was observed under identical conditions in the absence of TFA and TBAA (Figure 1g). Interestingly, Circular dichroism (CD) characterization suggested the formation of helical polypeptides during TFA/TBAA-accelerated polymerization (Figure S6), excluding the possibility that there was no conformational change in the presence of TFA and TBAA.

2.2 | Improved Control Over MWs Mediated by TFA/TBAA Cooperative System

Considerable efforts in recent years have provided catalyst systems that are highly active [19, 31, 39, 40] or highly selective [13, 41–44], yet it remains challenging to achieve both properties

simultaneously. A representative example is CCP, where the slow initiation relative to ultrafast propagation results in a significant deviation from the expected MWs, particularly at low $[M]_0/[I]_0$ [20, 21]. Consequently, the development of even faster CCP systems has been hindered by the inherent challenge of MW control. The TFA/TBAA cooperative system offers a promising strategy to overcome the rate/MW-control dilemma, as all propagating chains grew simultaneously at a high rate (Figure 1g). Gel permeation chromatography (GPC) traces exhibited monomodal distribution with narrow dispersity ($Đ < 1.05$) at $[TFA]_0/[I]_0 > 1$, yielding polypeptides with molecular weight (M_n = 21.9 kDa) close to the theoretical M_n (Figure 2a and Table S1). The well-controlled polymerization at higher $[TFA]_0/[I]_0$ ratios was attributed to the effective suppression of TBAA-mediated nucleophilic addition of carboxylate to C5-carbonyl on a NCA ring. In contrast, an insufficient amount of TFA ($[TFA]_0/[I]_0$ = 1) failed to inhibit this mechanism, thus resulting in an elevated MWs. As the second additive in this binary cooperative system, TBAA has been previously reported to initiate the rapid polymerization of NCA [19, 45]. Thus, we reasoned that the $[TBAA]_0/[TFA]_0$ ratio should show an impact on the MW control of the polymerization (Figure 2b and Table S2). An excess amount of TBAA ($[TBAA]_0/[TFA]_0$ = 2) led to broad molecular weight distribution (MWD), likely due to the fast initiation by TBAA which was remained in the system after conversion of TFA into AcOH (Figures S7 and S8 and Table S3). A decrease in the $[TBAA]_0/[TFA]_0$ ratio to 1.5 and 1 significantly improved control over the polymerization, owing to the proper alkalinity of the system, which would avoid the initiation from TBAA while maintaining its catalytic effect as proton shuttle complex. Therefore, an optimal ratio of $[I]_0/[TFA]_0/[TBAA]_0$ = 1:10:15 was identified and employed for all subsequent polymerizations to balance the high polymerization rate with precise molecular control.

TFA was commonly used to quench the polymerization as it protonates propagating amino groups, thus, it was never considered in the development of NCA polymerization. However, TFA has been confirmed crucial in the proposed TFA/TBAA cooperative system, which further prompted us to systematically study the impact of organic acids. Thereby, ROP of NCAs was conducted in the presence of acids with various pKa values (Figure 2c). The polymerization rate decreased progressively with the pKa of the acid (Figure S9). Only strong acids like TFA (pKa = 0.52) and methanesulfonic acid (MSA) (pKa = -1.2) yielded polypeptides with narrow dispersity and targeted MWs (Figure 2d,e and Table S4). It is noteworthy that both TFA and MSA inhibited polymerization in the presence of Hex-NH_2 (Figure S10), enabling simultaneous chain growth upon the addition of TBAA. In contrast, acids with relative higher pKa values led to broad dispersity (Figure 2d,e), likely due to their lower reactivity toward TBAA, which left a larger amount of TBAA in the system. The residual TBAA inevitably initiated the ROP of NCAs, yielding ill-defined polypeptides, which was confirmed by matrix-assisted laser desorption–ionization-time of flight (MALDI-TOF) mass spectrometry (Figure S11), with two end groups observed. On the contrary, only polymeric species initiated by Hex-NH_2 (123.18 + 219.1n ($[M + Na]^+$) and 123.18 + 219.1n + 112 ($[M + Na]^+$) were observed across all detected molecular weight ranges (Figure 2f,g and Table S5) in TFA/TBAA cooperative system, with no carboxylate end groups observed in the resulting polypeptides (Figure 2g and Table S5), suggesting that polypeptides were exclusively initiated by Hex-NH_2. Additionally, polymerization catalyzed by individual TBAA exhibited MWs that substantially deviated from the theoretical values (Figure S8 and Table S3), highlighting the essential synergistic role between TFA and TBAA, which enabled precise control over polymerization and solo initiation by Hex-NH_2.

With the encouraging initial results, we conducted systematic ROP studies under different monomer conversions and various $[M]_0/[I]_0$ ratios (ranging from 25 to 400). The linear correlation between MWs and monomer conversions suggested a living polymerization process (Figure 2h). Moreover, the obtained polypeptides at various $[M]_0/[I]_0$ ratios exhibited MWs agreeing well with theoretical values, with narrow dispersity observed for all polymerizations (Figure 2i and Table 1). Notably, the MWD of the polypeptides at $[M]_0/[I]_0 < 50$, which were more susceptible to non-simultaneous chain growth, was significantly improved in the presence of TFA and TBAA (Figure 2i and Table 1), substantiating the improved MW control of TFA/TBAA cooperative system. Though polypeptides synthesized at $[M]_0$ ranging from 0.1 M to 0.2 M exhibited predictable MWs and narrow dispersity ($Đ < 1.08$), a small secondary peak at higher elution time could be observed (Figures S5 and S12 and Table S6). An increase in $[M]_0$ to 0.3 M and 0.4 M led to the elimination of the secondary peak, likely due to their fast kinetics which outpaced side reactions, further suggesting a well-controlled polymerization process at higher $[M]_0$.

The accelerated, controlled polymerization in TFA/TBAA cooperative system was further extended to other monomers and initiators (Figure S13). Well-defined polypeptides were obtained from the polymerization of N^{ε}-carboxybenzyl-L-lysine NCA (ZLL-NCA), γ-ethyl-L-glutamate NCA (ELG-NCA) and γ-(4-propargyloxy)benzyl-L-glutamate NCA (POB-NCA) (Figure S13a,b and Table 1). POB-NCA has a functional alkyne side chain, enabling further modification via click chemistry. Other primary amines, including benzylamine, propargylamine, and methoxy poly(ethylene glycol) amine, were also used as initiator for TFA/TBAA-accelerated polymerization (Figure S13c,d and Table 1), yielding polypeptides with targeted MWs and narrow dispersity. The successful incorporation of the functional group at the C terminus allowed for further functionalization. Additionally, the living nature of TFA/TBAA cooperative system allowed for efficient chain extension to prepare block co-polypeptides. GPC characterization revealed a clear peak shift to higher MWs, indicating a high blocking efficiency (Figures 2j and S14; Tables 1 and S7).

To further explore the scope of applicable proton shuttle catalyst in this cooperative catalytic system, we investigated several alternatives to TBAA. First, we examined tertiary amines including TEA, *N*,*N*-diisopropylethylamine (DIPEA), and 4-dimethylaminopyridine (DMAP), which are known to promote proton transfer in dormant species (—NH_3^+). All these amines accelerated the polymerization, achieving 95% NCA conversion within 1 h (Figure S15). However, these tertiary amines resulted in ill-defined polypeptides with broad dispersity (Figure 2k and Table S8), likely due to their strong basicity which can promote side reactions via AMM. Meanwhile, the impact of

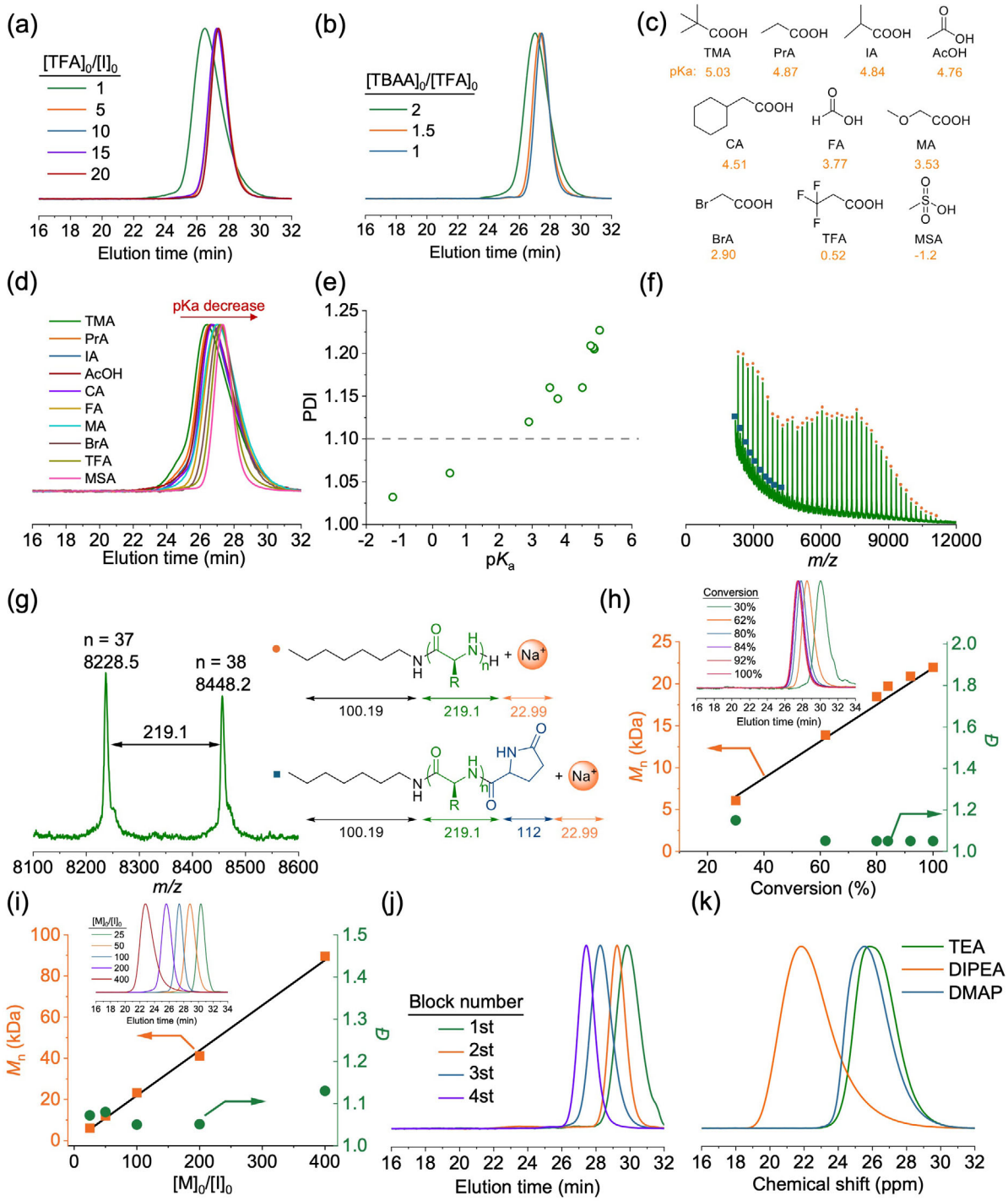

FIGURE 2 | Molecular weight control of TFA/TBAA cooperative system-accelerated polymerization. (a) Normalized GPC-LS traces of obtained poly(γ-benzyl-L-glutamate) (PBLG) at various $[TFA]_0$. $[M]_0/[I]_0/[TBAA]_0 = 100:1:15$, $[M]_0 = 0.3$ M. (b) Normalized GPC-LS traces of obtained PBLG at various $[TBAA]_0$. $[M]_0/[I]_0/[TFA]_0 = 100:1:10$, $[M]_0 = 0.3$ M. (c) Chemical structure of various organic acid with different pKa values. (d) Normalized GPC-LS traces of obtained PBLG from acid-TBAA accelerated polymerization in the presence of acid with different pKa. $[M]_0/[I]_0/[Acid]_0/[TBAA]_0 = 100:1:10:15$ and $[M]_0 = 0.3$ M. (e) The plot of polypeptide polymer dispersity index (PDI) against the pKa value of added organic acids. (f) MALDI-TOF characterization of PBLG obtained from TFA/TBAA-assisted polymerization. (g) The obtained m/z signals agree well with the calculated values of (123.18 + 219.1n) ($[M + Na]^+$) and (123.18 + 219.1n + 112), indicating negligible degradation of terminal amino groups. (h) The obtained MWs and dispersity at various monomer conversions during TFA/TBAA-assisted polymerization of BLG-NCA initiated by Hex-NH_2 in DCM. Inset: Normalized GPC-LS traces of obtained PBLG at various BLG-NCA conversions. $[M]_0/[I]_0/[TFA]_0/[TBAA]_0 = 100:1:10:15$, $[M]_0 = 0.3$ M. (i) The obtained MWs and dispersity of resulting PBLG initiated by Hex-NH_2 at different $[M]_0/[I]_0$ ratios in TFA/TBAA cooperative system. Inset: Normalized GPC-LS traces of obtained PBLG at different $[M]_0/[I]_0$ ratios. $[M]_0 = 0.3$ M, $[I]_0/[TFA]_0/[TBAA]_0 = 1:10:15$. (j) Normalized GPC-LS traces of the resulting PBLG initiated by Hex-NH_2 at various block numbers in TFA/TBAA cooperative system. (k) Normalized GPC-LS traces of obtained PBLG using different tertiary amines as proton shuttle catalyst. $[M]_0/[I]_0/[TFA]_0/[\text{Tertiary amine}]_0 = 100:1:10:15$.

TABLE 1 | Characterization of the resulting polypeptides from the polymerization of NCA monomers in TFA/TBAA cooperative system[a].

Entry	Monomer	Initiator	$[M]_0/[I]_0$	t (min)[b]	$M_{n,GPC}$ (kDa)[c]	$M_{n,theo.}$ (kDa)	$Đ$[c]
1	BLG-NCA	Hex-NH_2	25	3	6.0	5.5	1.07
2	BLG-NCA	Hex-NH_2	50	5	12.1	10.9	1.08
3	BLG-NCA	Hex-NH_2	100	10	23.3	21.9	1.03
4	BLG-NCA	Hex-NH_2	200	15	41.2	43.8	1.05
5	BLG-NCA	Hex-NH_2	400	25	89.6	87.6	1.13
6	ZLL-NCA	Hex-NH_2	100	10	30.9	26.2	1.12
7	POB-NCA	Hex-NH_2	100	10	27.3	26.8	1.06
8	ELG-NCA	Hex-NH_2	100	10	11.2	15.7	1.05
9	BLG-NCA	Propargylamine	100	10	22.2	21.9	1.02
10	BLG-NCA	Benzylamine	100	10	21.4	21.9	1.03
11	BLG-NCA	PEG_{5k}-NH_2	100	10	31.3	26.9	1.13
12[d]	BLG-NCA	Hex-NH_2	25/25/25/25	3/3/3/3	6.44/11.0/15.7/22.5	5.48/10.9/16.4/21.9	1.19/1.03/1.05/1.02

[a]All polymerizations were conducted in DCM in TFA/TBAA cooperative system at room temperature. $[M]_0 = 0.3$ M, $[I]_0/[TFA]_0/[TBAA]_0 = 1/10/15$.
[b]Polymerization time reaching 95% monomer conversion.
[c]Determined by GPC (*N*,*N*-dimethylformamide (DMF) containing 0.1 mol/L LiBr was used as the mobile phase). dn/dc = 0.1-0.123.
[d]Preparation of multiblock co-polypeptides through sequential addition of NCA monomers.

halide salts with structures analogous to TBAA was also studied, including tetrabutylammonium bromide (TBAB) and tetrabutylammonium iodide (TBAI). No polypeptide was detected after 24 h of polymerization (Figure S16), suggesting that neither TBAB nor TBAI could facilitate the transition of dormant species into active species. Therefore, TBAA, which contains the weakly acidic acetic conjugate group, proved to be unique and essential for achieving both high reactivity and controllability in this system.

2.3 | MW Control Mechanism in TFA/TBAA Cooperative System

The accelerated and controlled polymerization in TFA/TBAA cooperative system encouraged us to elucidate the underlying mechanism. We first monitored the reaction between TFA and TBAA in DCM. The acid displacement reaction proceeds via proton transfer from the strong acid (CF_3COOH, pKa ≈ 0.23) [46] to the acetate anion (CH_3COO^-, pKa ≈ 4.76) [46], generating AcOH and the corresponding trifluoroacetate salt, TBAF ($[(C_4H_9)_4N]^+[CF_3COO]^-$) (Figure 3a). Specifically, upon the addition of TBAA to a TFA solution, the proton signal of tetrabutylammonium cation shifted up-field (from 3.269 ppm to 3.242 ppm), consistent with the formation of TBAF (Figures 3b and S17). Concurrently, the signal assigned to the proton in the acetate anion shifted from 1.904 ppm to 2.037 ppm, suggesting the release of AcOH (Figure 3b). These observations collectively demonstrated that TFA reacted with TBAA, yielding TBAF and AcOH.

To further elucidate the mechanism, we quantify each species in the system using ^{1}H NMR. The presence of TBAA significantly influences the chemical shift of methyl group in AcOH (Figure S18a), while the presence of TBAF did not (Figure S19), suggesting that the change in chemical shift originates specifically from the interactions between AcOH and TBAA. We therefore conducted a systematic NMR titration of AcOH/TBAA mixtures, which showed a linear increase in the methyl chemical shift with AcOH content ($R^2 = 0.995$) (Figure S18b). Based on this, AcOH content was calculated to be 66.5% at $[M]_0/[I]_0/[TFA]_0/[TBAA]_0 = 100:1:10:15$ (Figure S20), corresponding to the generation of 9.98 equiv. of AcOH and the retention of 5.02 equiv of TBAA after the reaction of 10 equiv of TFA with 15 equiv of TBAA, accompanied by 9.98 equiv of in situ generated TBAF. In other words, 99.8% of TFA was converted to AcOH (Figure 3a). Similarly, 98.0% and 50.0% TFA were calculated to be converted into AcOH at $[M]_0/[I]_0/[TFA]_0/[TBAA]_0 = 100:1:10:10$ and 100:1:10:5, respectively (Table S9). The unconverted TFA in the system would lead to stable protonation of primary amines, thus decelerating the polymerization (Figure 1c).

The importance of each component after acid displacement (e.g., AcOH, TBAF and TBAA) was revealed by separate experiments. Before the addition of TBAA, TFA completely and irreversibly protonated the terminal amines, inhibiting polymerization by blocking nucleophilic attack (Figures S2 and S10). Whereas the addition of TBAA led to > 95% NCA consumption in 10 min, likely due to the conversion of inhibitory TFA into catalytic AcOH, which reversibly protonated the chain-end amines and initiated the polymerization (Scheme 1c) [33]. ^{1}H NMR analysis revealed that > 95% primary amino groups were protonated in the presence of individual TFA, as calculated from the integral area of the proton in -N$\boldsymbol{H}_3^+$ (Figure 3c,d). Moreover, the multiplicity of these methylene signals confirmed the complete protonation of Hex-NH_2, rationalizing the strong inhibitory effect of TFA (Figure 3d). Afterwards, the addition of TBAA converted TFA into AcOH, which significantly decreased the protonation of primary amino groups from ~ 95% to ~65% (Figure S21), and further increase in $[TBAA]_0/[TFA]_0$ ratio decreased protona-

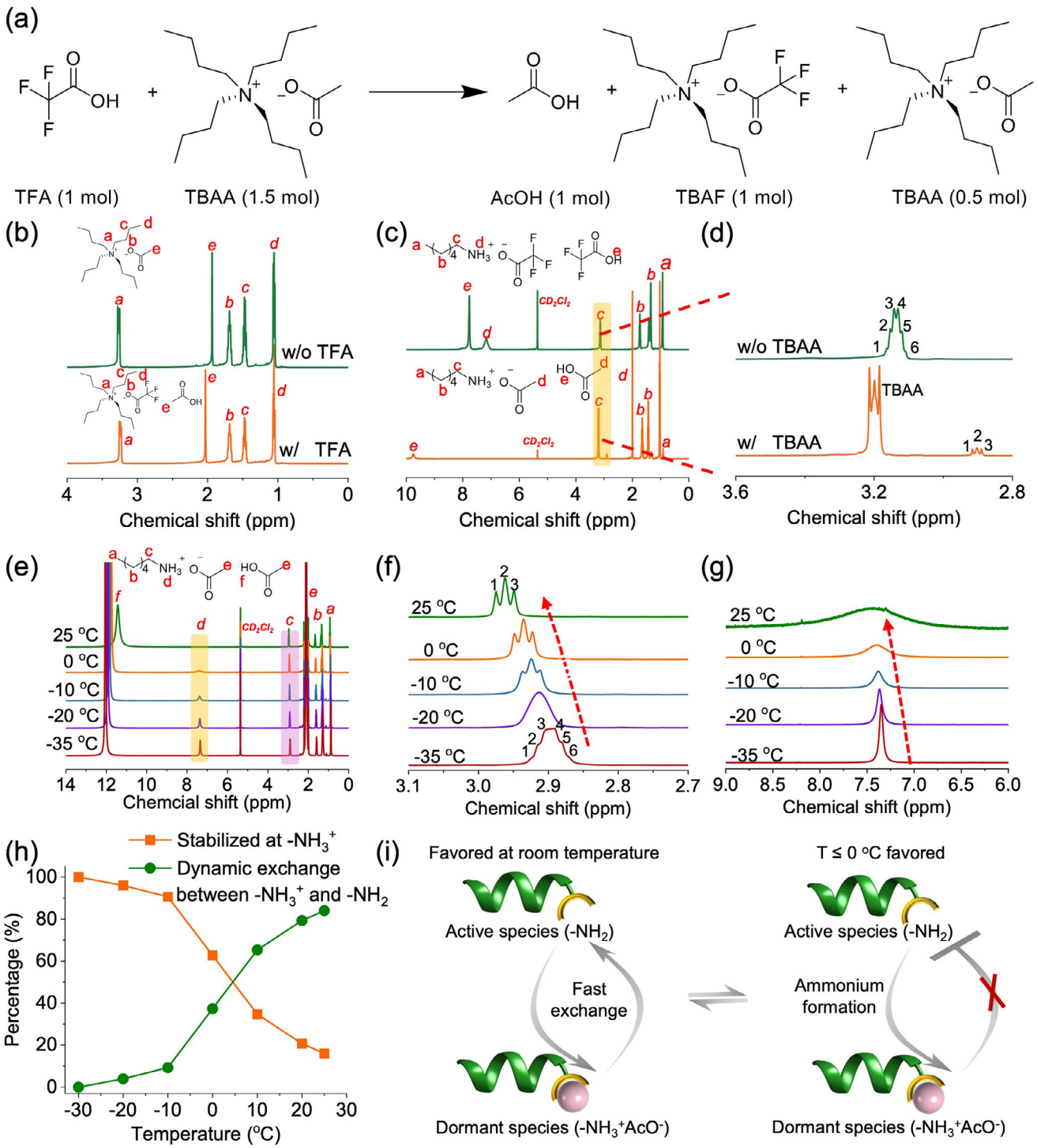

FIGURE 3 | Elucidation of the control mechanism in the TFA/TBAA cooperative system. (a) Theoretical reaction route of TFA and TBAA at $[TFA]_0/[TBAA]_0$ = 1:1.5, 1 equiv. of newly generated AcOH and TBAF, as well as 0.5 equiv. of unreacted TBAA will be contained in this system. (b) Overlaid ^1H NMR spectra of TBAA in CD_2Cl_2 in the absence and presence of TFA. $[TFA]_0/[TBAA]_0$ = 1:1.5. (c) Overlaid ^1H NMR spectra of the mixture of Hex-NH_2 and TFA in CD_2Cl_2 in the absence and presence of TBAA. $[I]_0/[TFA]_0/[TBAA]_0$ = 1:10:15. (d) Overlaid ^1H NMR spectra of α-H in Hex-NH_2 in the absence and presence of TBAA in CD_2Cl_2. $[I]_0/[TFA]_0/[TBAA]_0$ = 1:10:15. (e) Overlaid ^1H NMR spectra of the equilibrium system in Hex-NH_2 in the presence of AcOH in CD_2Cl_2 at different temperatures. (f) Overlaid ^1H NMR spectra of α-H in Hex-NH_2 in the presence of AcOH in CD_2Cl_2 at different temperatures. (g) Overlaid ^1H NMR spectra of dormant species (-N$\boldsymbol{H}_3^+$) from a stable existence state to a state of rapid and dynamic exchange. (h) Percentage of -NH_3^+ that existed stably and underwent rapid and dynamic exchange calculated from (g). (i) Scheme illustration showing the different interconversion that existed between active and dormant species at different temperatures.

tion degree to approximately 30% (Figure S21), with around 70% of the chain-ends were available for nucleophilic attack (Figures 3d and S21). Given that the equilibrium was governed by AcOH produced from the reaction between TFA and TBAA, we employed a minimal system comprising only Hex-NH_2 and AcOH to investigate the exchange between the dormant and active species via variable-temperature ^{1}H NMR spectroscopy. At -35°C, the equilibrium was effectively frozen, favoring the dormant species with the methylene group exhibiting a sextet signal in the presence of adjacent ammonium species. As the temperature increased, this signal gradually coalesced and transformed into a triplet peak, corresponding to the methylene group adjacent to the active free amine (Figure 3e,f). The protonation of Hex-NH_2 was further quantified by the integration of ammonium signals at various temperatures. The proportion of ammonium increased from 16% at 25°C to 100% at -35°C (Figure 3g,h), suggesting the temperature-dependent proton shuttle behavior. Additionally, the signal assigned to ammonium proton upfield shifted from 7.451 to 7.352 ppm upon cooling, demonstrating the increased population of protonated, dormant state (Figure 3g). The NMR analysis not only verified the existence of a rapid equilibrium in the TFA/TBAA cooperative system but also elucidated its critical role in achieving good control over the polymerization (Figure 3i).

2.4 | Proton Transfer Shuttle in TFA/TBAA Cooperative System

Moreover, the TFA/TBAA-catalyzed polymerization was investigated in various solvents. Well-controlled, accelerated polymerization of NCA occurred only in low-polarity solvents with weak hydrogen bonding capacity, such as DCM and chloroform (Figure 4a). Though polymerizations conducted in ethyl acetate (EA), tetrahydrofuran (THF) and DMF exhibited similar kinetics (Figure S22), the resulting polypeptides featured broad MWD (Figure 4a and Table S10). Given that pKa of the system was mediated by $[TFA]_0/[TBAA]_0$ ratios, we conducted polymerization in DMF at various $[TFA]_0/[TBAA]_0$ ratios to regulate pKa of the system. The resulting polypeptides exhibited broad dispersity and MWs deviated from theoretical value at all $[TFA]_0/[TBAA]_0$ ratios (Figure S23 and Table S11), indicating that varying $[TFA]_0/[TBAA]_0$ ratio was unable to improve control over polymerization.

Since there were strong solvating properties of EA, DMF and THF for both NCA monomers and growing polypeptide chains, the observed solvent dependence implies that specific molecular interactions, rather than general solvation, played a critical role in the TFA/TBAA-accelerated polymerization. In solvents with low polarity (like DCM and chloroform), AcOH was prone to interact with primary amines and form dormant species ($-NH_3^+CH_3COO^-$), establishing the dormant–active equilibrium for better MW control. Furthermore, AcOH would stabilize the nucleophilic carboxylate via hydrogen bonding, attenuating the initiation by TBAA (Figure 4b). TBAF would increase the concentration of fluorine-substituted carboxylate and quaternary ammonium cation, suppressing the dissociation of TBAA and consequently inhibiting its initiation. However, solvents with higher polarity would interfere with the above interactions between AcOH and primary amines/TBAA. These solvents tend to form hydrogen bonding interactions with AcOH, suppressing the formation of dormant species ($-NH_3^+CH_3COO^-$). The broken dormant–active equilibrium would lead to loss of control over the polymerization. Additionally, these solvents would also facilitate the dissociation of TBAA via stabilization of both ions through hydrogen bonding, retaining the initiation ability of TBAA. The initiation by both primary amine and TBAA would further lead to uncontrolled polymerization.

Another crucial aspect of NCA polymerization lies in increasing the fraction of active chain ends without compromising control over the rapid polymerization. Notably, the system retained 5.02 equiv. of TBAA alongside AcOH and TBAF (Table S9), which would promote the formation of active chain ends via proton transfer shuttle. To elucidate this process, we reconstructed the system in the model molecule experiment, containing Hex-NH_2, AcOH and TBAA. In the TBAA-free system, AcOH protonated approximately 48.3% of the Hex-NH_2 (Figure 4c–e). Strikingly, the addition of TBAA decreased the proportion of dormant ammonium end groups to about 30.0% (Figure 4c–e), owing to the proton shuttle between TBAA and AcOH. Briefly, nucleophilic TBAA attracted an equivalent of proton from dormant -NH_3^+ AcO^-, generating an active -NH_2 chain end and an equivalent of free AcOH. The remaining tetrabutylammonium cation would combine with the released acetate anion, resulting in the newly generated TBAA (Figure 4d). Although TBAA has been reported to rapidly initiate NCA ring-opening polymerization, the resulting polypeptides synthesized in DCM often exhibit significant deviations from the target MW (Figure 4f,g). This can be attributed to the initiation by the nucleophilic carboxylate anions of TBAA. In contrast, the TFA/TBAA cooperative system yielded polypeptides with molecular weights agreeing well with the theoretical values and narrow dispersity ($Đ$ <1.1) (Figure 4g). This controlled behavior is achieved through the function of in situ generated AcOH and TBAF: (1) AcOH and TBAF inhibited the initiation by TBAA; (2) AcOH interacted with both polypeptides adopting random-coiled and α-helical conformations, attenuating rate difference and achieving the one-stage polymerization.

Previous studies had identified the ROP between the active amine species and the NCA monomer as the rate-determining step (RDS), which is consistent with the experimentally observed first-order kinetics. To elucidate the effect of TBAA in proton transfer shuttle between dormant and active species, DFT calculations were carried out, focusing on model reactions between —NH_2 with AcOH, both in the presence and absence of TBAA (Figure 5). In individual AcOH-catalyzed systems, the concerted pathway was favored, with an activation free energy (ΔG) of 6.84 kcal/mol for transition states 1 (TS1), suggesting that the amine living center readily proceeded from intermediate 2 (INT2) (3.85 kcal/mol) to INT3 (-2.13 kcal/mol) through TS1, which led to the formation of dormant species (Figure 5a). TBAA inhibited the formation of dormant species (-NH_3^+) by altering the proton transfer pathway between AcOH to -NH_2. The mechanism began with TBAA disrupting the hydrogen bonding interaction between the carbonyl lone pair of an AcOH dimer (Figure 5b). The subsequent addition of -NH_2 led to the formation of INT2, which then must overcome a significant energy barrier to reach TS1. The energy required for this step (5.45 kcal/mol) substantially increased compared to the pathway without TBAA. More critically, the

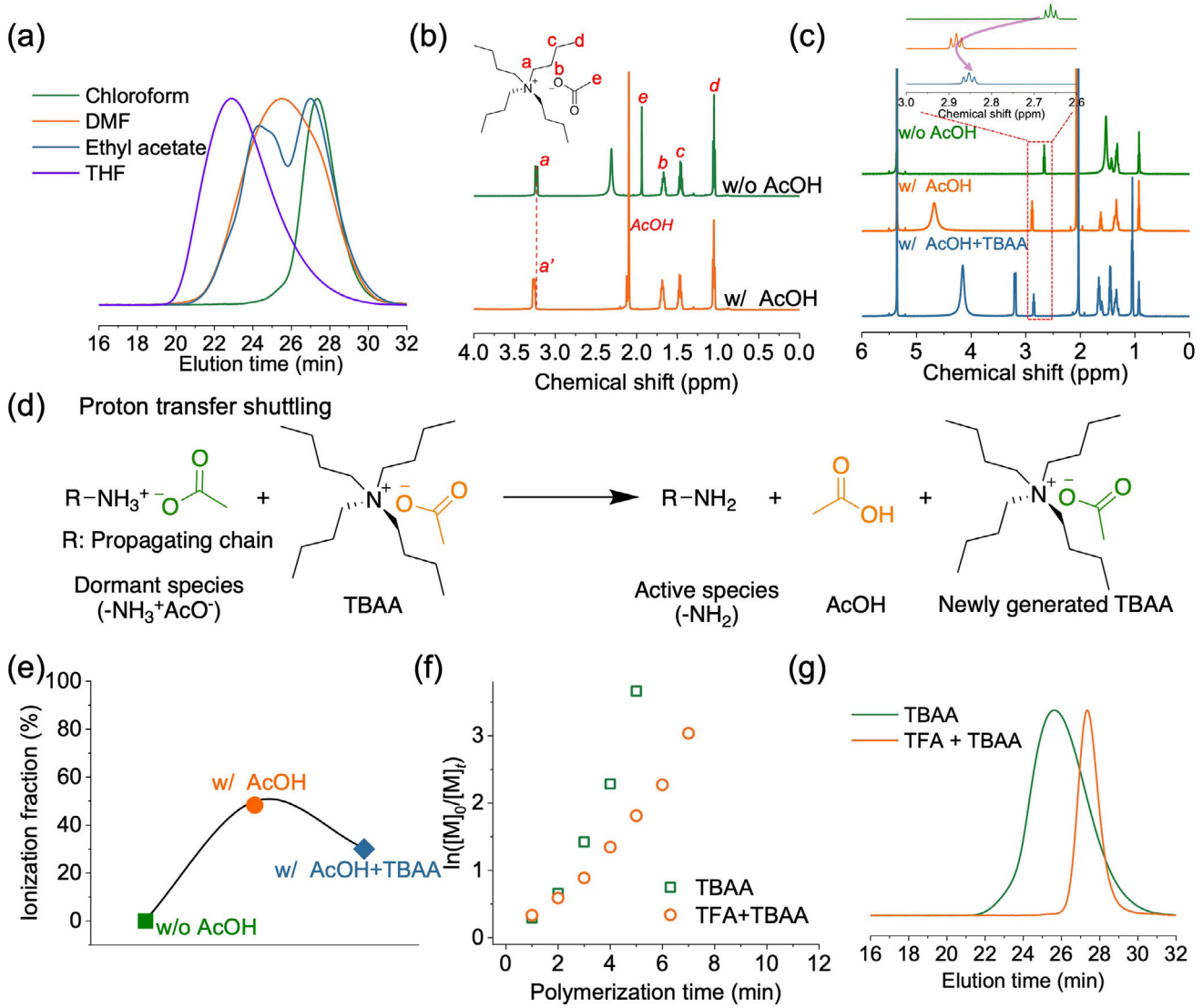

FIGURE 4 | TFA/TBAA cooperative system promotes the proton transfer shuttle between dormant species and active species. (a) Normalized GPC-LS traces of the obtained PBLG in various solvents initiated by Hex-NH_2 in TFA/TBAA cooperative system. $[M]_0/[I]_0/[TFA]_0/[TBAA]_0$ = 100:1:10:15, $[M]_0$ = 0.3 M. (b) Overlaid ^{1}H NMR spectra of TBAA in CD_2Cl_2 in the absence and presence of AcOH. $[TBAA]_0/[AcOH]_0$ = 5:10. (c) Overlaid ^{1}H NMR spectra of Hex-NH_2 in CD_2Cl_2 in the absence and presence of AcOH and TBAA. $[I]_0/[AcOH]_0/[TBAA]_0$ = 1:10:5. Inset: Overlaid ^{1}H NMR spectra showing the multiplicity of α-H of Hex-NH_2 in CD_2Cl_2 in the absence and presence of AcOH and TBAA. (d) Scheme illustration showing that TBAA attracts an equivalent of proton from dormant -$NH_3^+AcO^-$ to form active -NH_2 chain end. (e) The ionization fraction of Hex-NH_2 in the absence and presence of AcOH and TBAA. $[I]_0/[AcOH]_0/[TBAA]_0$ = 1:10:5. (f) Semilogarithmic kinetic plot of polymerization of BLG-NCA in DCM initiated by Hex-NH_2 in the presence and absence of TFA. $[M]_0/[I]_0/[TFA]_0/[TBAA]_0$ = 100:1:10:15, $[M]_0$ = 0.3 M. (g) Normalized GPC-LS traces of the resulting PBLG initiated by Hex-NH_2 in the presence and absence of TFA in DCM, $[M]_0/[I]_0/[TFA]_0/[TBAA]_0$ = 100:1:10:15, $[M]_0$ = 0.3 M.

overall energy barrier for the conversion from -NH_2 to -NH_3^+ (e.g., from INT2 to INT3) raised from -5.98 kcal/mol (without TBAA) to -2.86 kcal/mol (with TBAA) (Figure 5b), which made the formation of dormant species kinetically less favorable. TBAF was also found to have a similar function to TBAA in inhibiting the formation of dormant species (Figure S24). Additionally, we calculated the ionization degrees in different systems based on DFT calculations. Interestingly, the introduction of TBAA into the AcOH-catalyze system reduced the ionization degree from 99% to 91%, indicating a decrease in the concentration of acetate and -NH_3^+ species, and a corresponding increase in free acetic acid and -NH_2 proportion (Figure S25). This finding aligned well with the experimental results presented in Figure 4e, confirming that TBAA enhanced the polymerization rate by regulating proton transfer to maintain a higher concentration of active species.

In addition, in situ generated AcOH promoted the decarboxylation of carbamate species through a concerted eight-membered-ring transition state TS1. Compared to the previously reported TS1 without AcOH [33], the nearly linear proton-transfer geometry in AcOH-assisted TS1 (Figure S26a) is more favorable, resulting in a significantly lower $\Delta G‡$ of 3.94 kcal/mol. The energy of the decarboxylated intermediate INT3 was substantially lower than that of the carbamic-acid-containing intermediate INT1 (0 vs. -14.4 kcal/mol), indicating a thermodynamically favorable

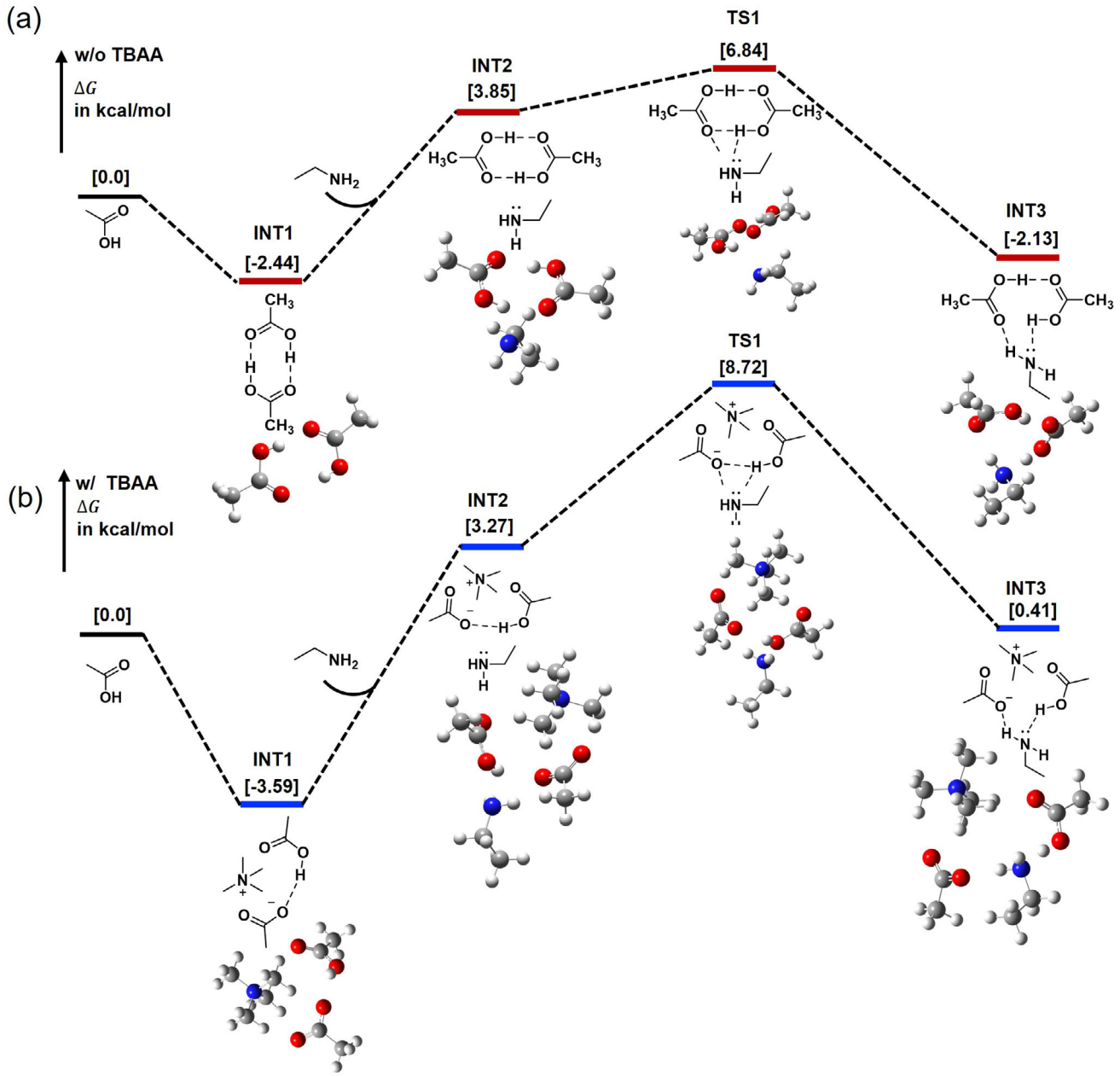

FIGURE 5 | Calculated Gibbs free energy profile of the model proton transfer shuttle process in the absence (a) and presence (b) of TBAA. Ethylamine and tetramethylammonium acetate were used as a model monomer for simplification. Some crucial intermediates (INT) and transition states (TS) are illustrated by 3D models where some hydrogen atoms are neglected for clarity.

decarboxylation in the presence of AcOH. The TFA/TBAA cooperative system featured the coexistence of newly generated AcOH and residual TBAA. To further examine the synergistic effect of AcOH and TBAA in the decarboxylation step, the intermolecular proton-transfer pathway was also evaluated via DFT calculations (Figure S26b). Compared to the case with individual AcOH, the involvement of TBAA further reduced the energy barrier $\Delta G‡$ from 3.94 kcal/mol to 3.08 kcal/mol. Moreover, the energy of INT3 in the presence of both AcOH and TBAA (-16.5 kcal/mol) is lower than that with individual AcOH (-14.4 kcal/mol), suggesting enhanced thermodynamic favorability in the presence of both. In summary, TFA and TBAA significantly accelerated ROP of NCAs by cooperatively catalyzing the decarboxylation step.

2.5 | Monomer Activation in TFA/TBAA Cooperative System

The activation of NCA monomer is another critical aspect of the polymerization mechanism. As previously reported, AcOH could facilitate the nucleophilic attack on NCA monomers for accelerated polymerization [33]. Thereby, we first investigated whether the accelerating effect of AcOH exists in this cooperative system. Indeed, the presence of AcOH induced a slight downfield shift of the ring N–H proton in BLG-NCA (from 6.36 ppm to 6.45 ppm), suggesting monomer activation by AcOH [47–50] (Figure S27). However, kinetic studies demonstrated that the TFA/TBAA cooperative system exhibited a faster polymeriza-

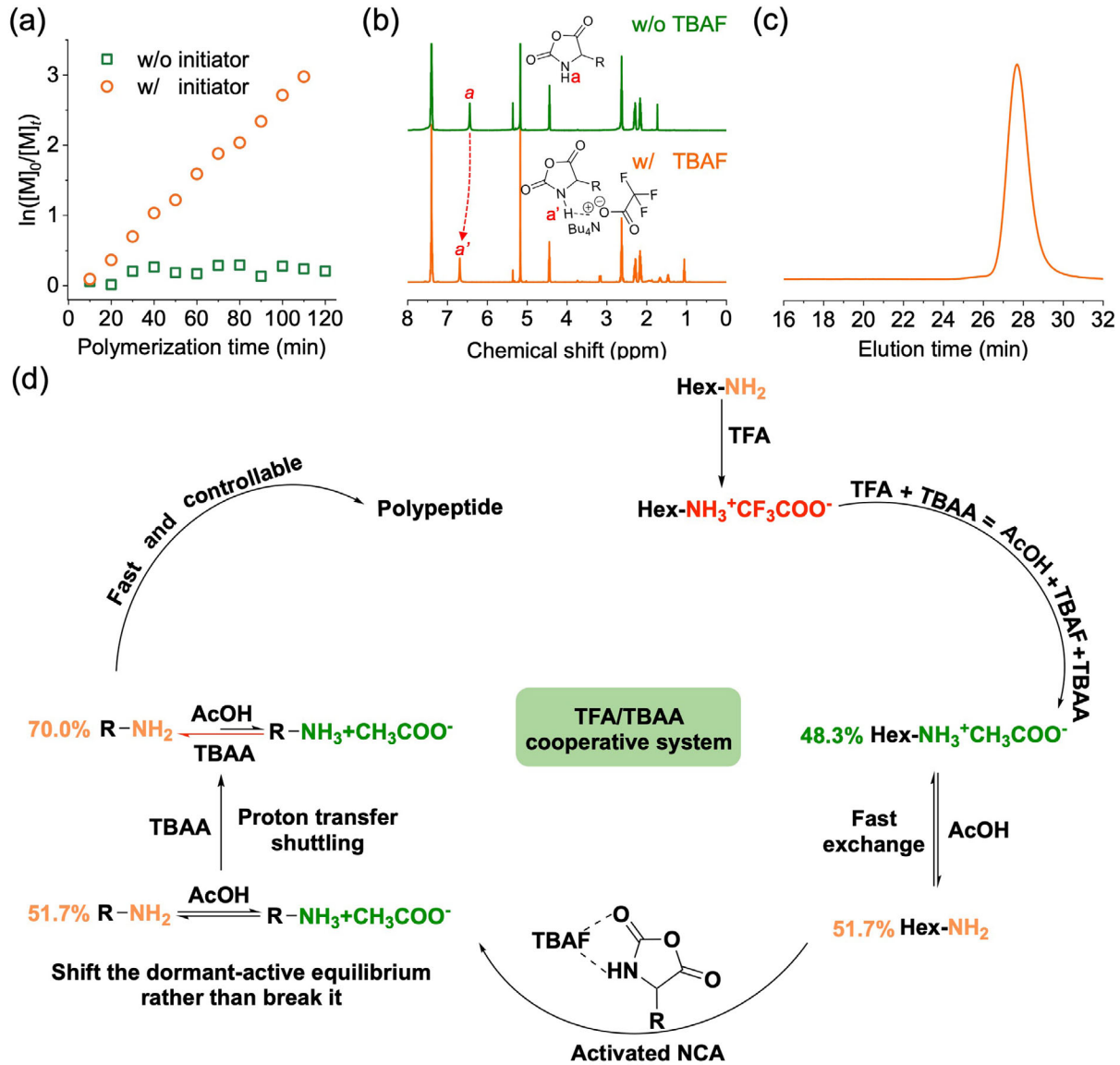

FIGURE 6 | Mechanism of ROP of NCA catalyzed by TFA/TBAA cooperative system. (a) Semilogarithmic kinetic plot of polymerization of BLG-NCA in DCM catalyzed by TBAF in the absence and presence of Hex-NH_2. $[M]_0/[I]_0/[TBAF]_0 = 100:1:10$. (b) Overlaid ^1H NMR spectra of BLG-NCA in the absence and presence of TBAF. $[BLG\text{-}NCA]_0/[TBAF]_0 = 10:1$. (c) Normalized GPC-LS traces of polymerization of BLG-NCA in DCM in the presence of Hex-NH_2, AcOH, TBAF and TBAA. $[M]_0/[I]_0/[AcOH]_0/[TBAF]_0/[TBAA]_0 = 100:1:10:10:5$, $[M]_0 = 0.3$ M. (d) Proposed mechanism for ROP of NCA catalyzed by TFA/TBAA cooperative system.

tion rate than an equivalent concentration of individual AcOH (Figure S28), suggesting that components other than AcOH must contribute to the activation of NCA monomers. A key additional component is the in situ-generated TBAF, the basicity of which is significantly reduced compared to its precursor TBAA, as it was associated with the strong acid TFA (Figure S29). Intriguingly, TBAF can facilitate monomer activation through hydrogen-bonding interactions with the NCA carbonyl groups, ultimately contributing to an accelerated ROP of NCA monomers (Figures 6a,b and S30). Meanwhile, TBAF, bearing an electron-withdrawing trifluoromethyl group, exhibits substantially weaker nucleophilicity compared to TBAA. Therefore, no detectable polymerization occurred after 120 min in the presence of individual TBAF (Figure 6a). To further confirm our hypothesis, we conducted the model experiment containing AcOH, TBAF and TBAA, as those existed after the reaction between TFA and TBAA in the proposed cooperative system. ROP of NCAs completed in just 10 min (Figure S31), and the resulting polypeptide exhibited predictable MW and narrow dispersity ($Đ < 1.05$) (Figure 6c), comparable to those synthesized in TFA/TBAA cooperative system. Therefore, each component is indispensable for achieving a rapid and controllable polymerization reaction.

The integrated DFT and experimental study establish the mechanism for the accelerated and controlled ROP of NCAs in the TFA/TBAA cooperative system (Figure 6d). Initially, TFA protonates the initiators (Hex-NH_2), forming dormant species (—$NH_3^+CF_3COO^-$) and effectively preventing premature initiation. The addition of TBAA triggers proton transfer between TFA and AcOH, converting inhibitory TFA into catalytic AcOH and restoring primary amines. The in situ generated AcOH reversibly protonates primary amines, establishing the equilibrium between

dormant species (ammonium salts) and active species (amino groups). Additionally, AcOH stabilizes the nucleophilic carboxylate of TBAA via hydrogen bonding (Figure 4b), suppressing unexpected TBAA-initiated pathways with no polymerization occurred within the first 10 min in the absence of initiator (Figure S32). Meanwhile, TBAF suppresses the dissociation of TBAA, decreasing the concentration of active carboxylate center and consequently inhibiting the initiation by TBAA (Figure S32). The dormant–active equilibrium, combined with the suppression of TBAA initiation pathways, allows for a controlled polymerization process. Furthermore, residual TBAA, which serves as a proton-transfer shuttle, shifts the equilibrium toward the active species, increasing the proportion of active chain ends from 51.7% to 70.0%. In situ generated AcOH and TBAF activates the incoming NCA monomer through hydrogen-bonding interactions. These two distinct mechanisms thereby collectively accelerate the polymerization. In summary, this TFA/TBAA cooperative strategy successfully modulates the delicate balance between basic/nucleophilic and acidic/electrophilic species, enabling rapid and controlled ROP of NCAs exclusively initiated by primary amines.

3 | Conclusion

This study reported the accelerated and controlled polymerization of NCA in a TFA/TBAA cooperative system under mild conditions. The methodology demonstrated a remarkable rate enhancement compared with non-catalyzed systems, yielding polypeptides with narrow MWD and enabling multiple chain extensions. Additionally, this polymerization exhibited good moisture tolerance, circumventing the stringent requirement for air-free conditions or dry solvents. ^{1}H NMR experiments and DFT calculations elucidated the critical role of TBAA as a regulator of dormant–active equilibrium. Specifically, TBAA was found to shift, rather than break this equilibrium, increasing the population of active chain ends from 51.7% to 70.0% and preserving MW control. This shift was attributed to an increased energy barrier for the formation of dormant species, which kinetically favored a higher concentration of active centers. Furthermore, AcOH and TBAF can, on the one hand, activate the NCA monomers, and on the other hand, inhibit the initiation by TBAA, collectively ensuring a rapid yet controlled ROP. The broad applicability of this method was suggested by its compatibility with various NCA monomers and initiators. In summary, this work not only enriched the fundamental understanding of controlled NCA polymerization and underscored the general importance of proton-shuttle mechanisms in ROP of NCA, but also provided a straightforward and robust strategy for synthesizing polypeptides with diverse MWs and application potentials.

Author Contributions

Jing Huang: methodology, investigation, writing – review and editing, writing – original draft, funding acquisition, conceptualization, resources. **Haonan Sheng:** methodology, software. **Jianjun Cheng:** writing – review and editing, conceptualization, project administration, writing – original draft, supervision, resources, methodology. **Xingliang Liu:** conceptualization, methodology, investigation, supervision, writing – review and editing, writing – original draft, funding acquisition, project administration, resources.

Acknowledgments

This work is supported by the National Natural Science Foundation of China (52503218 for X. Liu and 82502559 for J. Huang), Natural Science Foundation of Jiangsu Province (BK20251566), and the China Postdoctoral Science Foundation (2023M743133).

Conflicts of Interest

The authors declare no conflicts of interest.

Data Availability Statement

The data that supports the findings of this study are available in the supplementary material of this article.

References

1. H. R. Kricheldorf, "Polypeptides and 100 Years of Chemistry of α-amino Acid *N*-carboxyanhydrides," *Angewandte Chemie, International Edition* 45 (2006): 5752–5784, https://doi.org/10.1002/anie.200600693.

2. T. Leigh and P. Fernandez-Trillo, "Helical Polymers for Biological and Medical Applications," *Nature Reviews Chemistry* 4 (2020): 291–310, https://doi.org/10.1038/s41570-020-0180-5.

3. T. J. Deming, "Synthetic Polypeptides for Biomedical Applications," *Progress in Polymer Science* 32 (2007): 858–875, https://doi.org/10.1016/j.progpolymsci.2007.05.010.

4. K. Kataoka, A. Harada, and Y. Nagasaki, "Block Copolymer Micelles for Drug Delivery: Design, Characterization and Biological Significance," *Advanced Drug Delivery Reviews* 64 (2012): 37–48, https://doi.org/10.1016/j.addr.2012.09.013.

5. C. He, X. Zhuang, Z. Tang, H. Tian, and X. Chen, "Stimuli-Sensitive Synthetic Polypeptide-Based Materials for Drug and Gene Delivery," *Advanced Healthcare Materials* 1 (2012): 48–78, https://doi.org/10.1002/adhm.201100008.

6. J. Huang and A. Heise, "Stimuli Responsive Synthetic Polypeptides Derived From *N*-carboxyanhydride (NCA) Polymerisation," *Chemical Society Reviews* 42 (2013): 7373–7390, https://doi.org/10.1039/c3cs60063g.

7. C. Deng, J. Wu, R. Cheng, F. Meng, H.-A. Klok, and Z. Zhong, "Functional Polypeptide and Hybrid Materials: Precision Synthesis via α-amino Acid *N*-carboxyanhydride Polymerization and Emerging Biomedical Applications," *Progress in Polymer Science* 39 (2014): 330–364, https://doi.org/10.1016/j.progpolymsci.2013.10.008.

8. Z. Song, Z. Han, S. Lv, et al., "Synthetic Polypeptides: From Polymer Design to Supramolecular Assembly and Biomedical Application," *Chemical Society Reviews* 46 (2017): 6570–6599, https://doi.org/10.1039/C7CS00460E.

9. X. Zhou and Z. Li, "Advances and Biomedical Applications of Polypeptide Hydrogels Derived From α-amino Acid *N*-carboxyanhydride (NCA) Polymerizations," *Advanced Healthcare Materials* 7 (2018): 1800020, https://doi.org/10.1002/adhm.201800020.

10. A. Rasines Mazo, S. Allison-Logan, F. Karimi, et al., "Ring Opening Polymerization of α-amino Acids: Advances in Synthesis, Architecture and Applications of Polypeptides and Their Hybrids," *Chemical Society Reviews* 49 (2020): 4737–4834, https://doi.org/10.1039/C9CS00738E.

11. T. Melnyk, S. Đorđević, I. Conejos-Sánchez, and M. J. Vicent, "Therapeutic Potential of Polypeptide-Based Conjugates: Rational Design and Analytical Tools That Can Boost Clinical Translation," *Advanced Drug Delivery Reviews* 160 (2020): 136–169, https://doi.org/10.1016/j.addr.2020.10.007.

12. Y. Liu and L. Yin, "α-Amino Acid *N*-carboxyanhydride (NCA)-Derived Synthetic Polypeptides for Nucleic Acids Delivery," *Advanced Drug*

Delivery Reviews 171 (2021): 139–163, https://doi.org/10.1016/j.addr.2020.12.007.

13. T. J. Deming, "Facile Synthesis of Block Copolypeptides of Defined Architecture," *Nature* 390 (1997): 386–389, https://doi.org/10.1038/37084.

14. T. Aliferis, H. Iatrou, and N. Hadjichristidis, "Living Polypeptides," *Biomacromolecules* 5 (2004): 1653–1656, https://doi.org/10.1021/bm0497217.

15. G. J. M. Habraken, M. Peeters, C. H. J. T. Dietz, C. E. Koning, and A. Heise, "How Controlled and Versatile Is *N*-carboxy Anhydride (NCA) Polymerization at 0°C? Effect of Temperature on Homo-, Block- and Graft (co)Polymerization," *Polymer Chemistry* 1 (2010): 514–524, https://doi.org/10.1039/B9PY00337A.

16. Y. Liu, D. Li, J. Ding, and X. Chen, "Controlled Synthesis of Polypeptides," *Chinese Chemical Letters* 31 (2020): 3001–3014, https://doi.org/10.1016/j.cclet.2020.04.029.

17. W. Lv, Y. Wang, M. Li, X. Wang, and Y. Tao, "Precision Synthesis of Polypeptides via Living Anionic Ring-Opening Polymerization of N-Carboxyanhydrides by Tri-Thiourea Catalysts," *Journal of the American Chemical Society* 144 (2022): 23622–23632, https://doi.org/10.1021/jacs.2c10950.

18. N. Hadjichristidis, H. Iatrou, M. Pitsikalis, and G. Sakellariou, "Synthesis of Well-Defined Polypeptide-Based Materials via the Ring-Opening Polymerization of α-amino Acid *N*-carboxyanhydrides," *Chemical Reviews* 109 (2009): 5528–5578, https://doi.org/10.1021/cr900049t.

19. Y. Wu, K. Chen, X. Wu, et al., "Superfast and Water-Insensitive Polymerization on α-amino Acid *N*-carboxyanhydrides to Prepare Polypeptides Using Tetraalkylammonium Carboxylate as the Initiator," *Angewandte Chemie, International Edition* 60 (2021): 26063–26071, https://doi.org/10.1002/anie.202103540.

20. R. Baumgartner, H. Fu, Z. Song, Y. Lin, and J. Cheng, "Cooperative Polymerization of α-helices Induced by Macromolecular Architecture," *Nature Chemistry* 9 (2017): 614–622, https://doi.org/10.1038/nchem.2712.

21. Z. Song, H. Fu, R. Baumgartner, et al., "Enzyme-Mimetic Self-Catalyzed Polymerization of Polypeptide Helices," *Nature Communications* 10 (2019): 5470, https://doi.org/10.1038/s41467-019-13502-w.

22. Z. Song, H. Fu, J. Wang, et al., "Synthesis of Polypeptides via Bioinspired Polymerization of in Situ Purified N-carboxyanhydrides," *Proceedings of the National Academy of Sciences of the USA* 116 (2019): 10658–10663, https://doi.org/10.1073/pnas.1901442116.

23. W. Wang, H. Fu, Y. Lin, J. Cheng, and Z. Song, "Cooperative Covalent Polymerization of *N*-carboxyanhydrides: From Kinetic Studies to Efficient Synthesis of Polypeptide Materials," *Accounts of Materials Research* 4 (2023): 604–615, https://doi.org/10.1021/accountsmr.3c00046.

24. I. Dimitrov and H. Schlaad, "Synthesis of Nearly Monodisperse Polystyrene–Polypeptide Block Copolymers via Polymerisation of N-carboxyanhydrides," *Chemical Communications* (2003): 2944–2945, https://doi.org/10.1039/B308990H.

25. M. Meyer and H. Schlaad, "Poly(2-isopropyl-2-oxazoline)−Poly(l-glutamate) Block Copolymers Through Ammonium-Mediated NCA Polymerization," *Macromolecules* 39 (2006): 3967–3970, https://doi.org/10.1021/ma060523c.

26. B. Brulc, E. Žagar, M. Gadzinowski, S. Słomkowski, and M. Žigon, "Homo and Block Copolymers of Poly(β-benzyl-L-aspartate)s and Poly(γ-benzyl-L-glutamate)s of Different Architectures," *Macromolecular Chemistry and Physics* 212 (2011): 550–562, https://doi.org/10.1002/macp.201000710.

27. I. Conejos-Sánchez, A. Duro-Castano, A. Birke, M. Barz, and M. J. Vicent, "A Controlled and Versatile NCA Polymerization Method for the Synthesis of Polypeptides," *Polymer Chemistry* 4 (2013): 3182–3186, https://doi.org/10.1039/c3py00347g.

28. H. Tang and D. Zhang, "Solid state Self-Assembly of the Single-Walled Carbon Nanotubes and Poly(γ-benzyl-l-glutamate)s With Different Conformations," *Journal of Polymer Science Part A, Polymer Chemistry* 51 (2013): 4489–4497, https://doi.org/10.1002/pola.26856.

29. A. Doriti, S. M. Brosnan, S. M. Weidner, and H. Schlaad, "Synthesis of Polysarcosine From Air and Moisture Stable N-Phenoxycarbonyl-N-Methylglycine Assisted by Tertiary Amine Base," *Polymer Chemistry* 7 (2016): 3067–3070, https://doi.org/10.1039/C6PY00221H.

30. C. D. Vacogne and H. Schlaad, "Controlled Ring-Opening Polymerization of α-amino Acid N-carboxyanhydrides in the Presence of Tertiary Amines," *Polymer* 124 (2017): 203–209, https://doi.org/10.1016/j.polymer.2017.07.062.

31. W. Zhao, Y. Lv, J. Li, Z. Feng, Y. Ni, and N. Hadjichristidis, "Fast and Selective Organocatalytic Ring-Opening Polymerization by Fluorinated Alcohol Without a Cocatalyst," *Nature Communications* 10 (2019): 3590, https://doi.org/10.1038/s41467-019-11524-y.

32. C. D. Vacogne and H. Schlaad, "Primary Ammonium/Tertiary Amine-Mediated Controlled Ring Opening Polymerisation of Amino Acid *N*-carboxyanhydrides," *Chemical Communications* 51 (2015): 15645–15648, https://doi.org/10.1039/C5CC06905J.

33. X. Liu, J. Huang, J. Wang, et al., "Accelerated and Controlled Polymerization of *N*-carboxyanhydrides Assisted by Acids," *CCS Chemistry* 7 (2024): 2769–2780, https://doi.org/10.31635/ccschem.024.202403954.

34. S. Wang and H. Lu, "Unveiling Proton Transfer as the Key Process to Understand and Promote the Ring-Opening Polymerization of *N*-carboxyanhydrides," *Polymer Science Technology* 1 (2025): 76–81, https://doi.org/10.1021/polymscitech.4c00040.

35. Y. Hu, Z.-Y. Tian, W. Xiong, et al., "Water-Assisted and Protein-Initiated Fast and Controlled Ring-Opening Polymerization of Proline *N*-carboxyanhydride," *National Science Review* 9 (2022): nwac033, https://doi.org/10.1093/nsr/nwac033.

36. S. Wang, M.-Y. Lu, S.-K. Wan, et al., "Precision Synthesis of Polysarcosine via Controlled Ring-Opening Polymerization of *N*-carboxyanhydride: Fast Kinetics, Ultrahigh Molecular Weight, and Mechanistic Insights," *Journal of the American Chemical Society* 146 (2024): 5678–5692, https://doi.org/10.1021/jacs.3c14740.

37. W. Zhao, Y. Gnanou, and N. Hadjichristidis, "From Competition to Cooperation: A Highly Efficient Strategy towards Well-Defined (co)Polypeptides," *Chemical Communications* 51 (2015): 3663–3666, https://doi.org/10.1039/C4CC09055A.

38. M. Liao, Y. Yao, K. Gan, et al., "Self-Promoted Controlled Ring-Opening Polymerization via Side Chain-Mediated Proton Transfer for the Synthesis of Tertiary Amine-Pendant Polypeptoids," *Angewandte Chemie, International Edition* 64 (2025): e202417990, https://doi.org/10.1002/anie.202417990.

39. Y. Wu, D. Zhang, P. Ma, R. Zhou, L. Hua, and R. Liu, "Lithium Hexamethyldisilazide Initiated Superfast Ring Opening Polymerization of Alpha-Amino Acid *N*-carboxyanhydrides," *Nature Communications* 9 (2018): 5297, https://doi.org/10.1038/s41467-018-07711-y.

40. C. Chen, H. Fu, R. Baumgartner, Z. Song, Y. Lin, and J. Cheng, "Proximity-Induced Cooperative Polymerization in "Hinged" Helical Polypeptides," *Journal of the American Chemical Society* 141 (2019): 8680–8683, https://doi.org/10.1021/jacs.9b02298.

41. T. J. Deming, "Transition Metal-Amine Initiators for Preparation of Well-Defined Poly(γ-benzyl L-glutamate)," *Journal of the American Chemical Society* 119 (1997): 2759–2760, https://doi.org/10.1021/ja962625w.

42. T. J. Deming, "Amino Acid Derived Nickelacycles: Intermediates in Nickel-Mediated Polypeptide Synthesis," *Journal of the American Chemical Society* 120 (1998): 4240–4241, https://doi.org/10.1021/ja980313i.

43. T. J. Deming, "Cobalt and Iron Initiators for the Controlled Polymerization of α-amino Acid-*N*-carboxyanhydrides," *Macromolecules* 32 (1999): 4500–4502, https://doi.org/10.1021/ma9902899.

44. H. Lu and J. Cheng, "Hexamethyldisilazane-Mediated Controlled Polymerization of α-amino Acid *N*-carboxyanhydrides," *Journal of the*

American Chemical Society 129 (2007): 14114–14115, https://doi.org/10.1021/ja074961q.

45. Y. Wu, Y. Chen, H. Yu, A. Dong, and R. Liu, "Dual Functional Diblock Amino Acid Copolymer Displaying Synergistic Effect With Curcumin Against MRSA and Encapsulation of Curcumin," *Chinese Journal of Chemistry* 41 (2023): 3333–3338, https://doi.org/10.1002/cjoc.202300353.

46. A. Albert and E. P. Serjeant, in *The Determination of Ionization Constants: A Laboratory Manual*, ed. A. Albert and E. P. Serjeant (Springer, 1984), 136, https://doi.org/10.1007/978-94-009-5548-6.

47. N. E. Kamber, W. Jeong, R. M. Waymouth, R. C. Pratt, B. G. G. Lohmeijer, and J. L. Hedrick, "Organocatalytic Ring-Opening Polymerization," *Chemical Reviews* 107 (2007): 5813–5840, https://doi.org/10.1021/cr068415b.

48. M. K. Kiesewetter, E. J. Shin, J. L. Hedrick, and R. M. Waymouth, "Organocatalysis: Opportunities and Challenges for Polymer Synthesis," *Macromolecules* 43 (2010): 2093–2107, https://doi.org/10.1021/ma9025948.

49. C. Thomas and B. Bibal, "Hydrogen-Bonding Organocatalysts for Ring-Opening Polymerization," *Green Chemistry* 16 (2014): 1687–1699, https://doi.org/10.1039/C3GC41806E.

50. J. Xu, X. Wang, J. Liu, X. Feng, Y. Gnanou, and N. Hadjichristidis, "Ionic H-bonding Organocatalysts for the Ring-Opening Polymerization of Cyclic Esters and Cyclic Carbonates," *Progress in Polymer Science* 125 (2022): 101484, https://doi.org/10.1016/j.progpolymsci.2021.101484.

Supporting Information

Additional supporting information can be found online in the Supporting Information section.

Supporting Information is available and includes materials, instrumentations, detailed experimental methods, kinetic plot, NMR, FTIR, GPC, and CD data.

Supporting File 1: anie73389-sup-0001-SuppMat.docx.